Science Bulletin 69 (2024) 597–600

Contents lists available at ScienceDirect

Science Bulletin

journal homepage: www.elsevier.com/locate/scib

Short Communication

# Why chorus waves are the dominant driver for diffuse auroral precipitation

Xinliang Gao [a,b,1], Jiuqi Ma [a,b,1], Tong Shao [a,b], Rui Chen [a,b], Yangguang Ke [a,b], Quanming Lu [a,b,*]

[a] Deep Space Exploration Laboratory, School of Earth and Space Sciences, University of Science and Technology of China, Hefei 230026, China
[b] CAS Center for Excellence in Comparative Planetology, Hefei 230026, China

ARTICLE INFO

*Article history:*
Received 8 August 2023
Received in revised form 13 November 2023
Accepted 14 November 2023
Available online 16 December 2023



Earth's diffuse aurora (structureless auroras, 5–15 s pulsations and microbursts) occurs over a broad latitude range, which arises from the collision of energetic charged particles with atoms in the upper atmosphere [1]. Diffuse aurora exists for most of the time, and intensifies during geomagnetically active periods [2]. Although generally not visible to the naked eyes, it is the major source of energy input into the Earth's nightside upper atmosphere [3]. During magnetospheric substorms, ~100 eV to 1 keV plasmasheet particles are injected into the midnight sector magnetosphere. Due to the conservation of the particles' first two adiabatic invariants, the particles are energized to ~10–100 keV energies. A mechanism that violates the first adiabatic invariant of electrons is required to scatter them to enter the atmospheric loss cone (a small cone of angle ~3° wide at the equator) [4], through which electrons precipitate into the upper atmosphere and powering the diffuse aurora. The pitch angle scattering caused by interactions with plasma waves has been widely accepted [5,6].

Two distinct classes of magnetospheric plasma waves, electrostatic electron cyclotron harmonic (ECH) waves and electromagnetic whistler-mode chorus waves, are spontaneously excited by the loss cone/temperature anisotropy instability [7,8] of the injected plasma sheet electrons. Chorus is first detected at local midnight with the particle injection [9], and as the electron cloud drifts towards local dawn and beyond, chorus is generated at those local times as well. As both waves can resonate with electrons in the same energy range [10], it has been proposed that either one of them could scatter ~10–100 keV magnetospheric electrons [11]. Assuming independence of the ECH and chorus waves, previous theoretical studies [7,8] suggested that the wave growth rates are comparable in the inner magnetosphere, they have similar occurrence rate and intensity, thus contributing nearly equally to diffuse auroral precipitation. However, based on the wave measurement by Combined Radiation Release Experiment Spacecraft (CRRES), and the Fokker-Planck diffusion calculations, Thorne et al. [12] showed that the chorus waves are statistically more important than ECH waves in the inner magnetosphere, and that the chorus waves play the dominant role in scattering ~10–100 keV magnetospheric electrons.

The above-mentioned contradiction still is a big challenge. It is critical to fully understand why chorus waves take the dominant role in diffuse auroral precipitation. Based on the observations made by the Van Allen Probes (VAPs) [13], the Defense Meteorological Satellite Program (DMSP) [14], and Arase [15], together with particle-in-cell (PIC) simulations, we reveal the previously unseen fact that chorus waves can severely suppress ECH waves in the inner magnetosphere. This contradicts the traditional assumption that ECH and chorus waves are two independent classes of plasma wave [12]. These results indicate that the dominant role of chorus waves in diffuse auroral precipitation is a natural consequence of the interplay between the two waves.

On 16 December 2012, Van Allen Probe A was operating in the dawn sector during 3:00–6:00 MLT (magnetic local time) of the Earth's magnetosphere, near the magnetic equatorial plane (magnetic latitude ≈±0.6°), and at a radial distance of 5–6 $R_E$, where $R_E$ is the Earth's radius. A moderate substorm occurred at ~06:18 UT (universal time) with the geomagnetic auroral electrojet (AE) intensity of 163 nT, and the flux of energetic electrons (~10 keV) increased. As expected, both intense chorus and ECH waves are detected during the interval of 06:40–09:50 UT, falling in the frequency band below and above the electron gyrofrequency (~4000 Hz), respectively (Fig. 1b). The DMSP 16 [14] that measures the precipitating auroral electrons between 30 eV and 30 keV, was flying around the Earth at an altitude of ~850 km with an inclination of 98.9° (Fig. 1d). During two intervals, from 07:00 to

* Corresponding author.
*E-mail address:* qmlu@ustc.edu.cn (Q. Lu).
[1] These authors contributed equally to this work.

https://doi.org/10.1016/j.scib.2023.12.009
2095-9273/

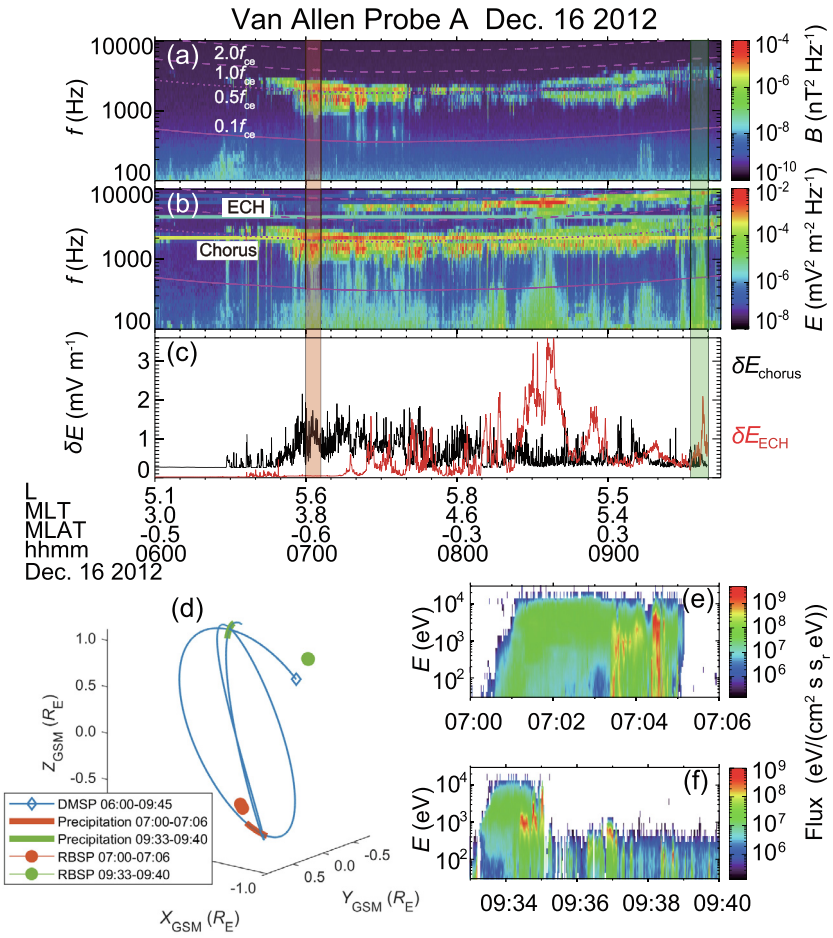


**Fig. 1.** Van Allen Probe A and DMSP 16 observations. (a, b) Wave magnetic field and electric field spectrograms, where $f_{ce}$ is the electron gyrofrequency. (c) The spectral intensity of chorus (black) and ECH waves (red). Two shaded regions mark the time intervals when the joint observations occur. (d) Locations of DMSP 16 and Van Allen Probe A in the Geocentric Solar Magnetic (GSM) coordinate. The solid blue line indicates the track of DMSP 16 during the interval of 06:00–09:45 UT, and the diamond represents its starting position. The circles represent the projected locations of Van Allen Probe A during the two shaded intervals, while the corresponding tracks of DMSP 16 are denoted by thick solid lines. $R_E$ is the Earth's radius. (e, f) Flux of precipitating electrons provided by DMSP 16.

07:06 UT, and from 09:33 to 09:40 UT (marked by shaded regions in Fig. 1d), the track of DMSP 16 was close to the footprint of Van Allen Probe A that has been mapped to the altitude of DMSP 16 based on Ts05 geomagnetic field model [16]. During 07:00–07:06 UT, the chorus waves have the dominant spectral intensity (~1.5 mV/m), but the ECH waves are negligible; while the reverse is true during 09:33–09:40 UT (Fig. 1c). We find that the flux of precipitating electrons in both time intervals is comparable and high, $\sim 10^9$ eV/(cm$^2$ s s$_r$ eV) in some short bursts (Fig. 1e, f). The precipitating electrons are mainly below ~10 keV, which can be contributed by either chorus or ECH waves. These observations demonstrate that either chorus waves or ECH waves can solely drive the significant diffuse auroral precipitation, in agreement with previous theoretical expectations [11]. There are also periods, like around 07:50 UT, when the electric amplitudes of the two waves are comparable. While the electron observation is not available for this period, we speculate that there will also be significant electron precipitations.

As shown in Fig. 1b, chorus and ECH waves are usually observed simultaneously as their source is the same [10], the ~10–100 keV magnetospheric electrons. However, their spectral intensities are inversely correlated with a cross-correlation coefficient of ~−0.5 (Fig. 1c). This feature was previously reported [12], but the importance has been missed. To reveal the global significance, we perform a statistical analysis of two-year VAPs spectrum data by selecting all chorus and ECH wave events (see Supplementary materials online). As expected, chorus and ECH waves preferentially occur in the nearly same region (Fig. 2a, b), from midnight to dawn (00:00–06:00 MLT), where the plasma sheet electrons are injected, adiabatically energized and then gradient and curvature drift eastward. However, chorus waves have much higher occurrence rate and intensity than ECH waves (Fig. 2a–d), consistent with previous observations. Therefore, it is natural to propose that ECH waves are strongly suppressed by chorus waves in the whole magnetosphere. To support this, we further classify all ECH wave events into three categories according to the intensity of simultaneous chorus waves. First, when chorus waves are very weak ($\delta E < 0.5$ mV/m), the occurrence rate and intensity of ECH waves are comparable to those in Fig. 2b, d (Fig. 2e, h), showing the majority of ECH wave events are observed under the condition that chorus waves do not gain sufficient growth. Second, when the intensity of chorus waves reaches the typical level ($0.5$ mV/m $< \delta E < 1.5$ mV/m) in the magnetosphere, there is a remarkable drop in the occurrence rate and intensity of ECH waves (Fig. 2f, i). Third, the intense ECH waves rarely occur when the intensity of chorus waves is larger than 1.5 mV/m (Fig. 2g, j).

The interpretation of the interplay between two waves is supported by the PIC simulation, in which we simulate their generation process by relaxing the anisotropic ~10–100 keV magnetospheric electrons with a loss-cone distribution

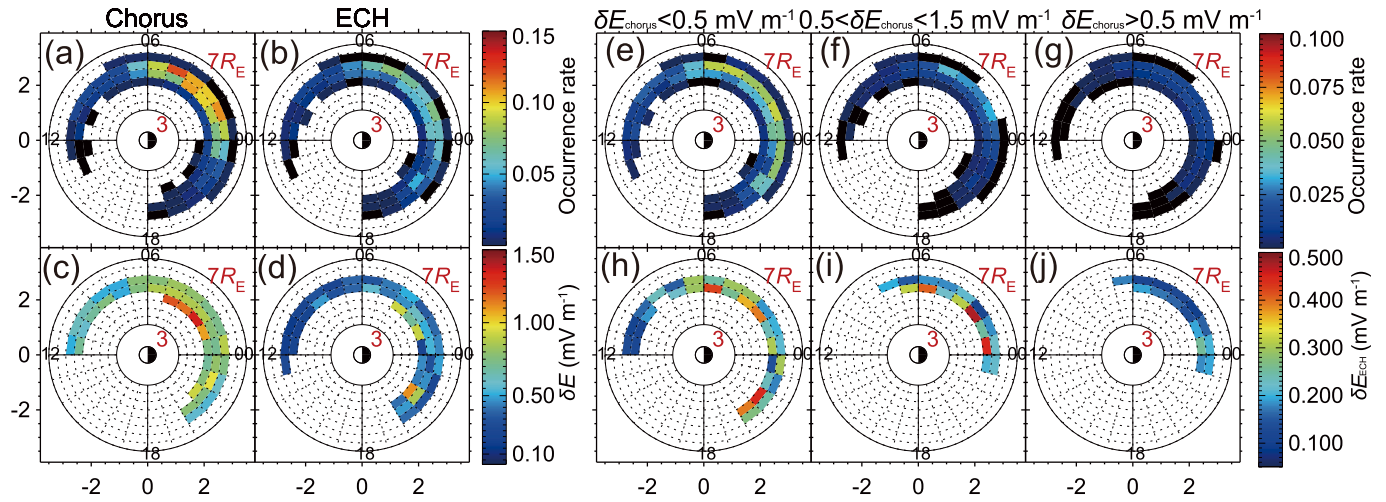


**Fig. 2.** Global distribution of chorus and ECH waves. (a–d) The statistical distribution of the occurrence rate (top) and average spectral intensity (bottom) of chorus waves and ECH waves in the L-MLT plane with the bin size of 0.5 L × 1 MLT. (e–j) The occurrence rate (top) and spectral intensity (bottom) of ECH waves in the L-MLT plane for different categories. The occurrence rate is defined as the ratio of the wave observation time to the satellite dwell time in the same category. The "00", "06", "12", and "18" represent MLT.

(see Supplementary materials online). To simplify the physical process, we do not involve the frequency chirping of whistler-mode chorus waves in this simulation. Generally, ECH waves are firstly excited from the background numerical noise even though chorus waves also have the comparable linear growth rate (~0.1 $\Omega_{ce}$), and reach the peak intensity early. In the early phase, the intense ECH waves can be observed with very weak whistler-mode waves, in analogy to the cases in Fig. 2e, f. Subsequently, ECH waves decay rapidly as whistler-mode waves grow until whistler-mode waves reach saturation (Fig. S1 online). It is shown that the loss cone has been significantly filled due to the growth of whistler-mode waves (Fig. S1 online), and the reshaped electron distribution causes the effective damping of ECH waves. The linear growth rate of ECH waves turns from positive to negative as the growth of whistler-mode waves. In the final phase, whistler-mode waves now become the dominant plasma wave, while ECH waves nearly drop to the noise level, consistent with the observations in Fig. 2g–j.

The Arase [15] satellite, equipped with a high-pitch angular resolution (i.e., 5°) electron analyzer, was flying eastward from 04:30 to 06:00 MLT on 30 March 2017. The intense ECH waves are firstly observed at ~17:00 UT with the spectral intensity of ~15.97 mV/m, and then gradually become weaker as chorus waves become stronger (Fig. S2 online). At ~19:00 UT, chorus waves are the dominant wave mode with the intensity of 14.21 mV/m, but ECH waves are too weak to observe (Fig. S2 online). The flux ratio between the loss-cone electrons and trapped electrons, quantifying the loss-cone shape of electron distribution, remains low during the interval of intense ECH waves since the loss-cone electron distribution provides the free energy for waves. As expected, the linear growth rate of ECH waves is positive during such interval. However, as chorus waves start to grow at ~17:25 UT, the flux ratio continues to increase due to the loss cone getting filled by scattered electrons. As a result, the linear growth rate of ECH waves turns negative (Fig. S2 online), and ECH waves are damped very rapidly.

These data uncover the long-neglected fact that chorus and ECH waves are closely related. Specifically, chorus waves can globally suppress ECH waves in the inner magnetosphere, leading to the much higher occurrence rate and intensity of chorus waves than ECH waves. The kinetic simulation reveals that ECH waves are generally excited early, but experience strong damping after the growth of whistler-mode chorus waves due to the rapidly reformed electron distribution, which is also supported by Arase data. Therefore, although either chorus or ECH waves can cause significant diffuse auroral precipitation, chorus waves must take the dominant role instead of ECH waves in the inner magnetosphere. Although chorus waves can also scatter electrons with higher energies (>~10 keV), the precipitating electrons contributing to the diffuse aurora are mainly below ~10 keV based on the DMSP observation. Therefore, the broader resonant energies for chorus waves will not affect the conclusion. Additionally, it should be noted that discrete auroras and the majority of precipitating electrons in the energy range of 100 eV to 10 keV result from acceleration in double layers [17], rather than through the wave-particle interactions. Recently Tsurutani et al. [5] have shown that chorus waves are typically coherent, which may imply that the growth rate calculations require an updated theory of chorus. In the outer magnetosphere ($L > 8$), since chorus waves generally have the relatively lower occurrence rate and intensity due to unfavorable plasma conditions, ECH waves can survive for very long time. As a result, ECH waves become more important in diffuse auroral precipitation in the outer magnetosphere [11]. This study represents an important step towards a complete physical understanding of Earth's and maybe other magnetized planetary diffuse aurora.

## Conflict of interest

The authors declare that they have no conflict of interest.

## Acknowledgments

This work was supported by the National Natural Science Foundation of China (42230201 and 42322406), the Strategic Priority Research Program of Chinese Academy of Sciences (XDB41000000), and "USTC Tang Scholar" Program. We also acknowledge the entire Van Allen Probes instrument teams.

## Author contributions

Xinliang Gao and Quanming Lu initiated the study and provided leadership for the project. Xinliang Gao and Jiuqi Ma carried out spacecraft data analysis and wrote the manuscript. Tong Shao performed simulations. Rui Chen participated in this research by

analyzing and interpreting simulations and observations. All authors contributed to editing the final manuscript.

## Appendix A. Supplementary materials

Supplementary materials to this short communication can be found online at https://doi.org/10.1016/j.scib.2023.12.009.

## Data availability

The entire Van Allen Probes dataset is publicly available at https://spdf.gsfc.nasa.gov/pub/data/rbsp/. The data from DMSP are obtained from https://spdf.gsfc.nasa.gov/pub/data/dmsp/dmspf16/ssj/. The Arase data are available from the EGR science center website (https://ergsc.isee.nagoya-u.ac.jp/data/ergsc/). The input parameters for the Ts05 magnetic model are available at http://geo.phys.spbu.ru/~tsyganenko/TS05_data_and_stuff/. All data supporting the findings of this study are available upon request.

## References

[1] Petrinec SM, Chenette DL, Mobilia J, et al. Statistical X ray auroral emissions—PIXIE observations. Geophys Res Lett 1999;26:1565–8.
[2] Jones AV. Aurora. Dordrecht-Holland: D. Reidel Publ. Co., 1974; p.35–39.
[3] Newell PT, Sotirelis T, Wing S. Diffuse, monoenergetic, and broadband aurora: The global precipitation budget. J Geophys Res Space Phys 2009;114:A09207.
[4] Schulz M, Lanzerotti LJ. Particle diffusion in the radiation belts. New York: Springer; 1974.
[5] Tsurutani BT, Verkhoglyadova OP, Lakhina GS, et al. Properties of dayside outer zone chorus during HILDCAA events: Loss of energetic electrons. J Geophys Res 2009;114:A03207.
[6] Kennel CF, Petschek HE. Limit on stably trapped particle fluxes. J Geophys Res 1966;71:1–28.
[7] Li W, Thorne RM, Meredith NP, et al. Evaluation of whistler mode chorus amplification during an injection event observed on CRRES. J Geophys Res 2008;113:A09210.
[8] Liu X, Chen LJ, Gu WY, et al. Electron cyclotron harmonic wave instability by loss cone distribution. J Geophys Res Space Phys 2018;123:9035–44.
[9] Tsurutani BT, Smith EJ. Postmidnight chorus: A substrom phenomenon. J Geophys Res 1974;79:118–27.
[10] Anderson RR, Maeda K. Vlf emissions associated with enhanced magnetospheric electrons. J Geophys Res Space Phys 1977;82:135–46.
[11] Ni BB, Thorne RM, Zhang XJ, et al. Origins of the Earth's diffuse auroral precipitation. Space Sci Rev 2016;200:205–59.
[12] Thorne RM, Ni BB, Tao X, et al. Scattering by chorus waves as the dominant cause of diffuse auroral precipitation. Nature 2010;467:943–6.
[13] Mauk BH, Fox NJ, Kanekal SG, et al. Science objectives and rationale for the radiation belt storm probes mission. Space Sci Rev 2013;179:3–27.
[14] Redmon RJ, Denig WF, Kilcommons LM, et al. New DMSP database of precipitating auroral electrons and ions. J Geophys Res Space Phys 2017;122:9056–67.
[15] Miyoshi Y, Shinohara I, Takashima T, et al. Geospace exploration project ERG. Earth Planets Space 2018;70:101.
[16] Tsyganenko NA, Sitnov MI. Modeling the dynamics of the inner magnetosphere during strong geomagnetic storms. J Geophys Res Space Phys 2005;110:A03208.
[17] Tsurutani BT, Zank GP, Sterken VJ, et al. Space plasma physics: A review. IEEE Trans Plasma Sci 2023;51:1595–655.

Xinliang Gao is an associate professor of School of Earth and Space Sciences, University of Science and Technology of China. He received his bachelor and Ph.D. degrees from University of Science and Technology of China in 2010 and 2015. His research interest focuses on the wave-particle interactions and shock waves in space.

Jiuqi Ma currently is pursuing a Ph.D. degree at the Deep Space Exploration Laboratory, School of Earth and Space Sciences, University of Science and Technology of China. Her research interest focuses on plasma waves in the magnetosphere and the solar wind.

Quanming Lu is a professor of school of Earth and Space Sciences, University of Science and Technology of China. He received his bachelor degree from Nanjing University in 1990 and Ph.D. degree from University of Science and Technology of China in 1996. His research interest focuses on magnetic reconnection and wave-particle interactions in space environment.